A New Method for Indoor-outdoor Image Classification Using Color Correlated Temperature

A. Nadian Ghomsheh *a_nadian@sbu.ac.ir*
Electrical and Computer Engineering Department
Shahid Beheshti University
Tehran, 1983963113, Iran

A. Talebpour *talebpour@sbu.ac.ir*
Electrical and Computer Engineering Department
Shahid Beheshti University
Tehran, 1983963113, Iran

Abstract

In this paper a new method for indoor-outdoor image classification is presented; where the concept of Color Correlated Temperature is used to extract distinguishing features between the two classes. In this process, using Hue color component, each image is segmented into different color channels and color correlated temperature is calculated for each channel. These values are then incorporated to build the image feature vector. Besides color temperature values, the feature vector also holds information about the color formation of the image. In the classification phase, KNN classifier is used to classify images as indoor or outdoor. Two different datasets are used for test purposes; a collection of images gathered from the internet and a second dataset built by frame extraction from different video sequences from one video capturing device. High classification rate, compared to other state of the art methods shows the ability of the proposed method for indoor-outdoor image classification.

Keywords: Indoor-outdoor Image Classification, Color Segmentation, Color Correlated Temperature

1. INTRODUCTION

Scene classification problem is a big challenge in the field of computer vision [1]. With rapid technological advances in digital photography and expanding online storage space available to users, demands for better organization and retrieval of image data base is increasing. Precise indoor-outdoor image classification improves scene classification and allows such processing systems to improve the performance by taking different methods based on the scene class [2]. To classify images as indoor-outdoor, it is common to divide an image into sub-blocks and process each block separately, benefiting from computational ease. Within each image sub-block, different low-level features such as color, texture, and edge information are extracted and used for classification.

Color provides strong information for characterizing landscape senses. Different color spaces have been tested for scene classification. In a pioneer work [3], an image was divided into 4×4 blocks, and Ohta color space [4]was used to construct the required histograms for extracting color information. Using only color information they achieved a classification accuracy of 74.2%. LST color space used by [5] achieved a classification accuracy of 67.6%. [6] used first order statistical features from color histograms, computed in RGB color space, and achieved a classification rate with 65.7% recall and 93.8% precession. [7] compared different features extracted from color histograms. These features include: opponent color chromaticity histogram, color correlogram [8], MPEG-7 color descriptor, colored pattern appearance histogram [9], and layered color indexing [10].Results of this comparison showed that no winner could be selected for all types of images but significant amount of redundancy in histograms can be removed. In [11] mixed channels of RGB, HSV, and Luv color spaces were incorporated to calculate color histograms. First and second order statistical moments of each histogram served as significant features for indoor-outdoor classification. To improve

classification accuracy, camera metadata related to capture conditions was used in [12]. In [13], each image was divided into 32×24 sub-blocks and a 2D color histogram in Luv color space along with a composite feature that correlates region color with spatial location derived from H component in HSV color space where used for indoor-outdoor image classification. [14, 15] proposed Color Oriented Histograms (COH) obtained from images divided into 5 blocks. They also used Edge Oriented Histograms (EOH) and combined them together to obtain CEOH as the feature to classify images into indoor-outdoor classes.

Texture and Edge features were also used for indoor-outdoor image classification. [5] extracted texture features obtained from a two-level wavelet decomposition on the L-channel of the LST color space[16]. In [17] each image was segmented via fuzzy C-means clustering and the extracted mean and variance of each segment represented texture features. [18] used variance, coefficient of variation, energy, and entropy to extract texture features for indoor-outdoor classification. Texture orientation was considered in [19]. From the analysis of indoor and outdoor images, and images of synthetic and organic objects, [20] observed that organic objects have a larger amount of small erratic edges due to their fractal nature. The synthetic objects, in comparison, have edges that are straighter, and less erratic.

Although color has shown to be a strong feature for indoor-outdoor image classification, dividing images into different blocks regardless of the information present in each individual image will degrade the classification results, as the mixture of colors in each block would be unpredictable. Another thing that has not gained much attention is the scene illumination where the image was captured in. This is an important aspect since indoor and outdoor illuminations are quite different and incorporating such information can effectively enhance the classification results.

To overcome such limitations when color information is considered for indoor-outdoor image classification, a new method based on the Color Correlated Temperature feature (CCT) is proposed in this paper. As will be shown, the apparent color of an object will change when the scene illumination changes. This feature can be very effective for the aims of this paper, since the illuminants of indoor scenes are much different compared to outdoor scenes. CCT is a way to show the apparent color of an image under different lighting conditions. In this process, each image is divided into different color segments and CCT is found for each segment. These values form the image feature vector, where, other than CCT information, color formation of the image is inherently present in the feature vector. In the classification phase KNN classifier is used for classification [21]. The focus of this paper is on the ability of color information for indoor-outdoor image classification. Edge and texture features can also be added to the image to enhance the classification rate, but this is beyond the scope of this paper.

The reminder of the paper is organized as follows: section 2 reviews the theory of color image formation in order to provide insight to why the concept of CCT can be effective for the aims of this research. In section 3 the proposed method for calculating the temperature vector for an arbitrary image is explained. Section 4 shows the experimental results, and section 5 concludes the paper.

2. REVIEW OF COLOR IMAGE THEORY

A color image is result of light illuminating the scene, the way objects reflect the light hitting their surfaces, and characteristics of the image-capturing device. In the following subsections, first, Dichromatic Reflection Model (DRM) is described and then various light sources are briefly looked at to show differences among them. This explanation shows why the concept of CCT can be utilized for indoor-outdoor image classification.

2.1 Dichromatic Reflection Model

A scene captured by a color camera can be modeled by spectral integration. This is often described by DRM. Light striking a surface of non-homogeneous materials passes through air and contacts the surface of the material. Due to difference in mediums index of refraction, some of the light will reflect from the surface of the material which is called surface reflectance (Ls). The light that penetrates into the body of the material is absorbed by the colorant, transmitted through the material, or will re-emit from the entering surface. This

component is called the body reflectance (Lb). [22]. The total light (L), reflected from an object is the sum of surface and body reflectance, and can be formulized as;

$$L(\lambda,\Omega) = L_s(\lambda,\Omega) + L_b(\lambda,\Omega) \quad (1)$$

where, λ is the wavelength of the incident light and Ω the photometric angle that includes the viewing angle e, the phase angle g, and the illumination direction angle i (fig.1). Ls and Lb are both dependent on the relative spectral power distribution (SPD), defined by Cs and Cb, and a geometric scaling factor ms and mb which can be formulized by;

$$L_s(\lambda,\Omega) = m_s(\Omega)C_s(\lambda) \quad (2)$$

$$L_b(\lambda,\Omega) = m_b(\Omega)C_b(\lambda) \quad (3)$$

Cs and Cb are also both product of the incident light spectrum (E), and the material's spectral surface reflectance (ρS) and body reflectance (ρB), defined by;

$$C_s(\lambda) = E_s(\lambda)\rho_s(\lambda) \quad (4)$$

$$C_b(\lambda) = E_b(\lambda)\rho_b(\lambda) \quad (5)$$

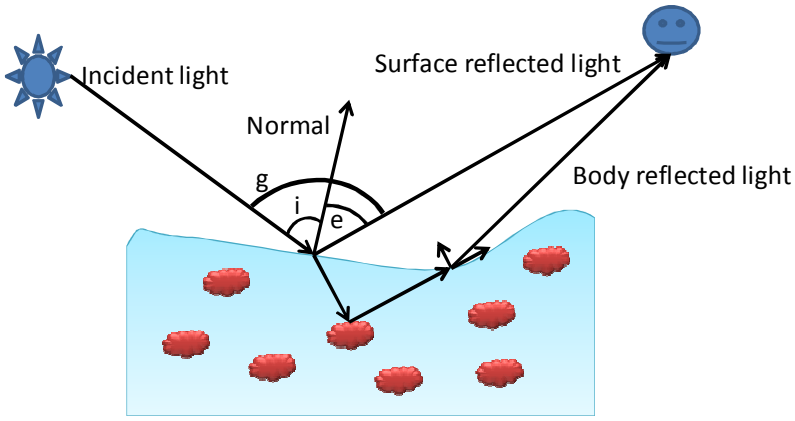

FIGURE 1: DRM model, showing surface reflectance and body reflectance from surface of an object.

By inspecting equations, (2) to (5) it can be observed that the light that enters into the camera is dependent on the power spectrum of the light source; therefore, for the same object different apparent color is perceived under different illuminations. Due to this fact, it can be implied that different groups of illuminants give an object different perceived colors. The less within class variance among a group of light sources and the more between class variance among different groups of light sources indicate a better distinguishing feature for indoor outdoor image classification when scene illumination is considered. In the next subsection different light sources are reviewed to how different classes of light sources differ from each other.

2.2- Light Sources

The color of a light source is defined by its spectral composition. The spectral composition of a light source may be described by the CCT. A spectrum with a low CCT has a maximum in the radiant power distribution at long wavelengths, which gives the material a reddish appearance, e.g. sunlight during sunset. A light source with a high CCT has a maximum in the radiant power distribution at short wavelengths and gives the material a bluish appearance, e.g., special fluorescent lamps [23]. Fig 2-a shows three fluorescent lamp SPDs compared with a halogen bulb, and Fig 2-b shows SPD of daylight in various hours of day. Comparison between these two types shows how the spectrums of fluorescents lamps follow the same pattern and how they are different with respect to the halogen lamp.

Fig. 2-c shows three diverse light spectrums; Blackbody radiator, a fluorescent lamp, and daylight all having a CCT of 6200 K. It can be seen that the daylight spectrum is close to the Blackbody spectrum whereas the fluorescent lamp spectrum deviates significantly from the blackbody spectrum.172 light sources measured in [24] showed that illuminant chromaticity

falls on a long thin band in the chromaticity plane which is very close to the Planckian locus of Blackbody radiators

By reviewing the SPDs of various light sources it can be implied that the same group of light sources show the same pattern in their relative radiant power when compared to other groups. This distinguishing feature makes it possible to classify a scene based on scene illuminant; which in this paper is incorporated for indoor-outdoor image classification.

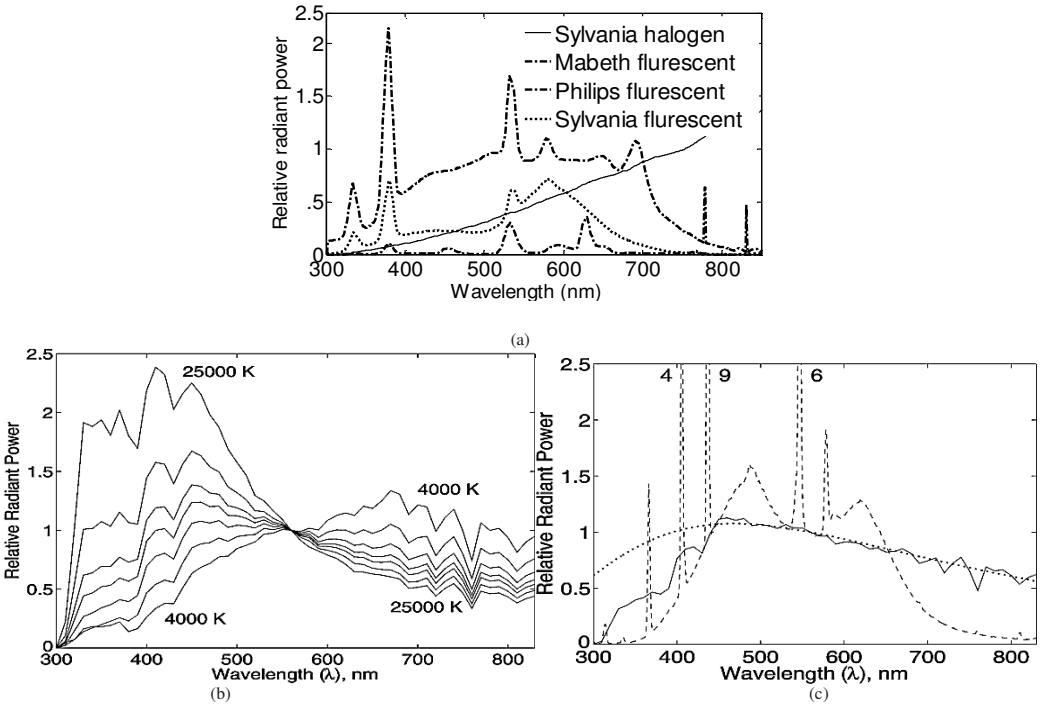

FIGURE 2: Different light sources with their SPDs. (a) SPDs for three different fluorescent lamps compared to SPD of halogen bulb [23]. (b) Daylight SPDs at different hours of day, normalized at 560nm. (c) Spectra of different light sources all with a CCT of 6200K and normalized at λ = 560 nm [24].

3. PROPOSED METHOD

Review of color image formation showed that the color of an image captured by the camera is result of the reflected light from the surface of objects as a sum of body and surface reflectance (eq. 1). Surface reflectance has same properties of the incident light and it is a significant feature for detecting the light source illuminating the scene. Body reflectance on the other hand most closely resembles the color of the material taking into account the spectra of the incident light; which in this paper is used as a metric to classify images as indoor and outdoor. Different steps of the proposed algorithm are shown in fig. 3.

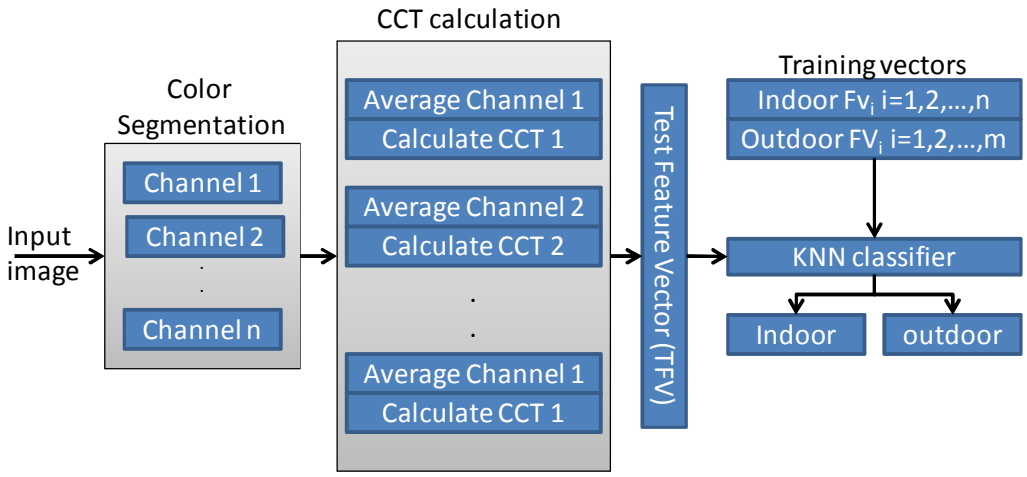

FIGURE 3: Block Diagram of the proposed method for indoor-outdoor classification

In the first step, color segmentation is performed and the image is partitioned into N color channels (each color segment is thought of an independent color channel). Next CCT is calculated for each channel, and the feature vector obtained is used for indoor-outdoor image classification. Finally a KNN classifier is used to partition images into two classes of indoor and outdoor. Each step of the algorithm is next explained in detail.

3.1 Color Segmentation

Many color spaces have been used for color segmentation. HSV is nonlinear color spaces and a cylindrical-coordinate representation of points in RGB color model. The nonlinear property of this color space makes it possible to segment colors in one color component independent of other components which is an advantage over linear color spaces [25]. This is color space is used here to segment images into desired number of segments; where each segment is called a "color channel". HSV is obtained from RGB space by:

$$h=\begin{cases}0 & if\ \max=\min\\ \left(60^\circ\times\dfrac{g-b}{\max-\min}\right)\bmod 360^\circ & if\ \max=r\\ 60^\circ\times\dfrac{b-r}{\max-\min}+120^\circ & if\ \max=g\\ 60^\circ\times\dfrac{r-g}{\max-\min}+240^\circ & if\ \max=b\end{cases} \quad (6)$$

$$s=\begin{cases}0 & if\ \max=0\\ 1-\min/\max & otherwise\end{cases} \quad (7)$$

$$v=\max \quad (8)$$

here max and min are the respective maximum and minimum values of r, g, and b, the RGB color components for each pixel in the image.

The following steps show how each image is converted to its corresponding color channels (*Ch*).For an input image with color components: Red, Green, and Blue:

1) Convert image from RGB color space to HSV
2) Quantize H component to 2^n where *n=1,2,…,N*
3) Find a mask that determines each color channel (*ch*):

$$if\ H(x,y)=n \quad mask_n(x,y)=1$$
$$else \quad mask_n(x,y)=0$$

4) Each *Ch* is then obtained by:

$$Ch_n=[(mask_n.red),(mask_n.Green),(mask_n.Blue)]$$

where "." Represent point-by-point multiplication of matrixes. After dividing each image into the respective color channels, CCT for each available channel has to be calculated.

3.2 Calculating CCT

A few algorithms have been introduced to estimate temperature of a digital image for scene classification or finding scene illumination[26, 27]. Different purpose of the previous algorithms makes them impractical for the aim of this paper.

Planckian, or blackbody locus can by calculated by colorimetrically integrating the Planck function at many different temperatures, with each temperature specifying a unique pair of chromaticity coordinates on the locus [28]. Inversely if one has the Planckian locus, then CCT can be calculated for every chromaticity coordinate. To find the CCT for each color channel it is necessary to find a chromaticity value to represent each color channel. The algorithm proposed for calculation CCT for each color channel has the following steps:

1) From V component of HSV color space, discard dark pixels that their value is smaller than 10% of maximum range of V for each *ch*.
2) Take average of the remaining pixels in RGB color space to discard surface reflectance through the iterative process.
3) Find the CCT of the color channel using the average chromaticity value.

From the DRM model it will be straight forward that dark pixels in the image do not hold information about the scene luminance since they are either not illuminated, or the reflected light from their surface does not enter the camera. In steps 2, pixels, which their values hold information mainly about surface reflectance, are discarded through an iterative process. In this process instead of just discarding bright points, the algorithm discards pixels with respect to luminance of other pixels. Using this average value, the CCT of each color channel is the calculated.

3.2.1 Calculating Average Chromaticity of L_b

The aim of averaging each channel is to discard pixels that have been exposed to direct light, or where the reflection from object's surface is in line with camera lenses. The value of such pixels may vary with respect to the surface reflectance and lighting condition. The flow chart to implement the proposed algorithm is shown in Fig. 4.

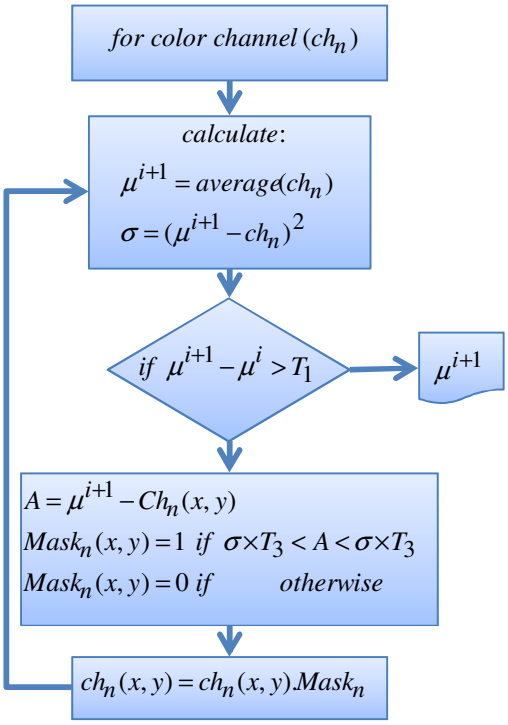

FIGURE 4: Different steps of color segmentation process

In this algorithm, *Ch(x,y)* is pixel value at position *(x,y)* in Ch_n, *M* is the mask that discards the unwanted information. "." is the inner product. σ is variance, and μ is the mean value of the remaining pixels in iteration *i*. *T1*, *T2*, and *T3* are the thresholds that have to be determined. The convergence of this algorithm is guaranteed since in worth case only one pixel of the image will be left unchanged and the calculated μ for that pixel will stay constant. Therefore, thresholds *T1*, *T2*, and *T3* can be chosen arbitrary. However, to find a good set of thresholds they are found by training them on 40 training images. To do so it is desired to find triple $T=(T_1,T_2,T_3)$ that for each color channel the best average point is obtained. This point is defined as "the point where the average values that is most frequently occurred". Let each $Ch_{i,n,C}$ be all the training color channels:

$$ch_{i,n,C} = \begin{bmatrix} ch_{1,1,1} & \cdots & ch_{1,n,1} \\ \vdots & \begin{bmatrix} ch_{1,1,2} & \cdots & ch_{1,n,2} \\ \vdots & & \\ ch_{i,1,2} & \begin{bmatrix} ch_{1,1,3} & \cdots & ch_{1,n,3} \\ \vdots & \ddots & \vdots \\ ch_{i,1,3} & \cdots & ch_{i,n,3} \end{bmatrix} \end{bmatrix} \\ ch_{i,1,} & & \end{bmatrix} \quad (9)$$

where *i (i=1,2,…,I)* is the number of image samples, *n (n= 1,2,…,N)* is the number of color channel in each image, and *C (C=1,2,3)* shows Red, Green, and Blue components. Also let T_1, T_2, and T_3 be vectors:

$$T_1 = [1.05, 1.1, ..., 1.3]$$
$$T_2 = [1.1, 1.2, ..., 1.5]$$
$$T_3 = [1, 2, ..., 5],$$

which can take the form:

$$T(\alpha) = \left\{ (T_1^1 T_2^1 T_3^1), (T_1^1 T_2^1 T_3^2), ..., (T_1^6 T_2^6 T_3^5) \right\} \quad (10)$$

where α=*1,2,…,180*. Set *T*(α) consists of all threshold combinations that have to be checked in order to find the best choice of thresholds, $\boldsymbol{T^{opt}}$. For each sample *Ch*, the average value of the channel in the respective color component is calculated for *T*(α), and stored in the average vector ***Avg***:

$$\boldsymbol{Avg}(\alpha) = [Avg(T(1)), Avg(T(2)),..., Avg(T(180))] \quad (11)$$

Next, the histogram of ***Avg*** with ten bin resolution is calculated (Fig. 5). The most frequent bin is considered as the acceptable average values of the *Ch* defined by Avg_{max}. Set T^{opt} shows the thresholds that yield Avg_{max} for a certain *Ch*, and is defined as:

$$T^{opt} = \arg\max_{T(\alpha)} \boldsymbol{Avg}(T(\alpha)) \quad (12)$$

By calculating T^{opt} for all color channels a set $T^{opt}(t)$, t=1,2,…,960 is achieved which can be written as:

$$T^{obt}(t) = \left\{ \underset{t_{red}=1:320}{T^{opt}{}_{red}}, \underset{t_{green}=321:640}{T^{opt}{}_{Green}}, \underset{t_{blue}=641:960}{T^{opt}{}_{blue}} \right\} \quad (13)$$

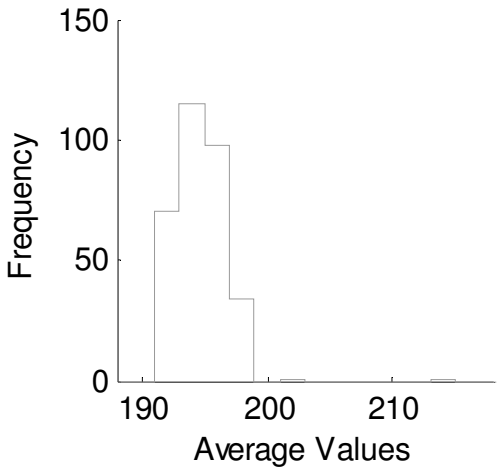

FIGURE 5: Finding different T that yield Avgmax

From this set it is possible to find the optimum thresholds for each color component, for example for the red channel $T^{opt,red}$, can be written as:

$$T^{obt,red} = \arg\max_{t_{red}} T^{opt}{}_{red}(t)` \quad (14)$$

$T^{obt,green}$ and $T^{opt,blue}$ are calculated in the same way as (14), and from them all the trained thresholds are obtained as:

$$\boldsymbol{T^{obt}} = \begin{bmatrix} T_1^{obt,red} & T_1^{obt,green} & T_1^{obt,blue} \\ T_2^{obt,red} & T_2^{obt,green} & T_2^{obt,blue} \\ T_3^{obt,red} & T_3^{obt,green} & T_3^{obt,blue} \end{bmatrix} \quad (15)$$

After calculating the average chromaticity value μ, it is possible to find the CCT of each Ch_n.

3.2.2 Calculating CCT For The Average Chromaticity

To calculate the CCT of a chromaticity value $\mu(x,y)$, it is transformed into Luv color space [25], where pixel μ is represented by coordinates (u,v). Fig 6 shows the Luv chromaticity plane with the plankian locus showing various Color temperatures, the perpendicular lines on the locus are iso-temperature lines.

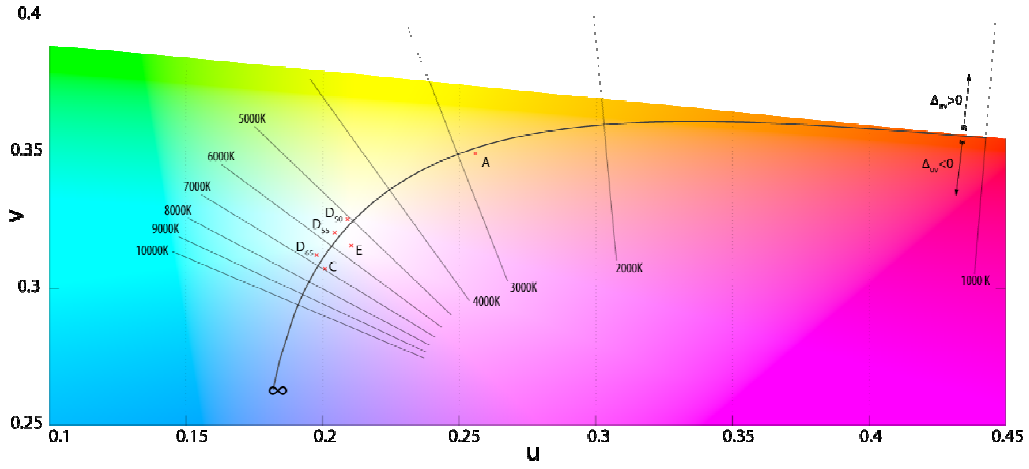

FIGURE 6: Luv chromaticity plane with the plankian locus.

By utilizing iso-temperature line CCT can be found by interpolation from look-up tables and charts. The most famous such method is Robertson's [29] (Fig 7). In this method CCT of a chromaticity value T_c, can be found by calculating:

$$\frac{1}{T_c} = \frac{1}{T_1} + \frac{\theta_1}{\theta_1 + \theta_2}\left(\frac{1}{T_i} - \frac{1}{T_{i+1}}\right) \tag{16}$$

where, θ is the angle between two isotherms. T_i and $T_{i+1}$are the color temperatures of the look-up isotherms and i is chosen such that $T_i<T_c<T_{i+1}$ (fig 7). If the isotherms are tight enough, it can assumed that, $(\theta_1/\theta_2)\approx(\sin\theta_1/\sin\theta_2)$, leading to:

$$\frac{1}{T_c} = \frac{1}{T_1} + \frac{d_i}{d_i - d_{i+1}}\left(\frac{1}{T_i} - \frac{1}{T_{i+1}}\right) \tag{17}$$

d_i is distance of the test point to the *i'th* isotherm given by:

$$d_i = \frac{(v_c - v_i) - m_i(u_c - u_i)}{\sqrt{1 + m_i^2}} \tag{18}$$

where, (u_i,v_i) is the chromaticity coordinates of the *i'th* isotherm on the Planckian locus and m_i is the isotherm's slope. Since it is perpendicular to the locus, it follows that $m_i=-1/l_i$ where l_i is the slope of the locus at (u_i,v_i). Upon calculation of CCT for all color channels, the feature vector *fv* containing the respective CCT for each color channel is obtained:

$$fv = [CCT_1, CCT_2, ..., CCT_N] \tag{19}$$

where, N is the number of color channels in each image. This vector can now be used for classification. In the classification phase, KNN classifier is used for classification. K is a user-defined constant, and the test feature vectors are classified by assigning the label which is most frequent among the K training samples nearest to that test point.

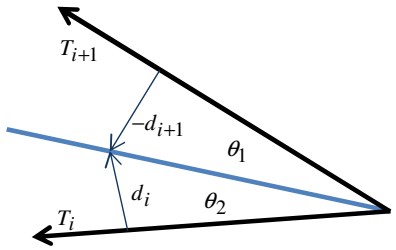

FIGURE 7: Robertson method for finding CCT of a chromaticity value.

4. EXPERIMENTAL RESULTS

To assess the performance of the proposed method, some tests are conducted on two sets of indoor and outdoor images. First a collection 800 images gathered from the internet named DB1 and a second dataset selected by extracting 800 frames from several video clips captured by a Sony HD handy cam (DB2).

Using DB2 it is possible to denote that camera effects are the same for all images; hence the classification ability of the proposed method is evaluated regardless of camera calibrations. A total of 40 clips captured in outdoors, and 25 different clips captured indoor were used to make DB2. The clips were captured at 29.97 frames per second and data were stored in RGB color space with 8bit resolution for each color channel. Fig 8 shows some sample indoor and outdoor frames. To show the difference between normal averaging and the averaging process introduced in this paper where the effect of surface reflectance is eliminated fig 9 is utilized.

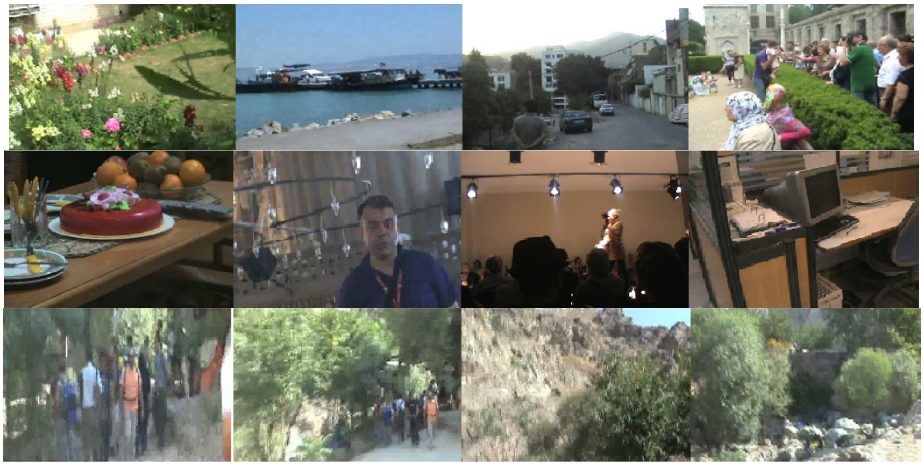

FIGURE 8: Top and middle rows: 4 indoor and outdoor and Bottom row: 4 consecutive outdoor frames

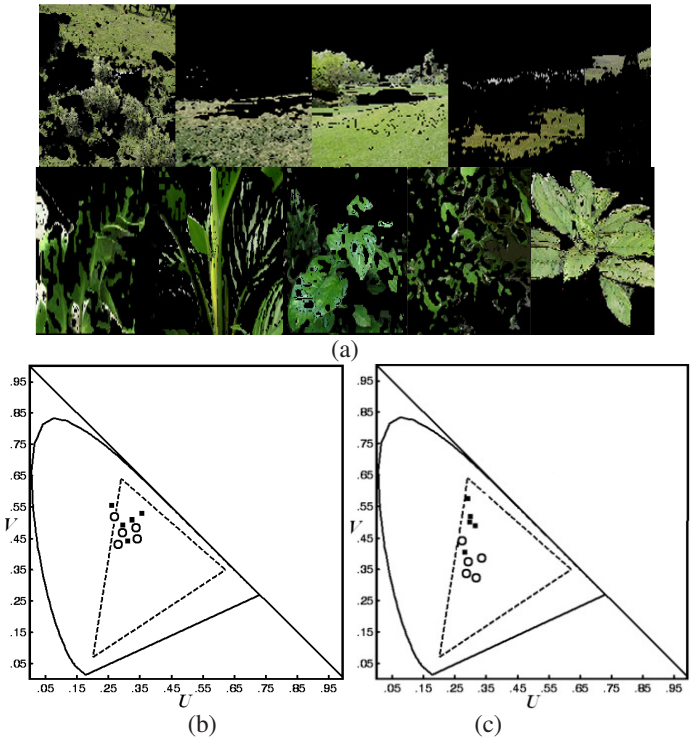

FIGURE 9: An example of the proposed algorithm for averaging color channels. a) Green channels of pictures taken in outdoor (top row) and at indoor situations (bottom row). (b) Normal averaging of the pixels. (c) Averaging pixels by the proposed algorithm.

Fig 9.a shows ten green color channels from five outdoor and five indoor scenes. For each color channel the corresponding average chromaticity value in the *uv* plane is shown. Outdoor images are shown with circles and indoor images are shown with black squares. As it can be seen when the effect of surface reflectance is obscured, the indoor and outdoor images are significantly separable. To calculate the average points T^{opt} was trained. The histogram of average values obtained for channel $Ch_{1,1,1}$ (as an example) are shown in fig10. Based on the histograms calculated for all different channels, the matrix $\boldsymbol{T^{opt}}$ was obtained as:

$$T^{opt} = \begin{bmatrix} 2 & 1 & 1 \\ 1.1 & 1.2 & 1.1 \\ 1.4 & 1.4 & 1.3 \end{bmatrix}$$

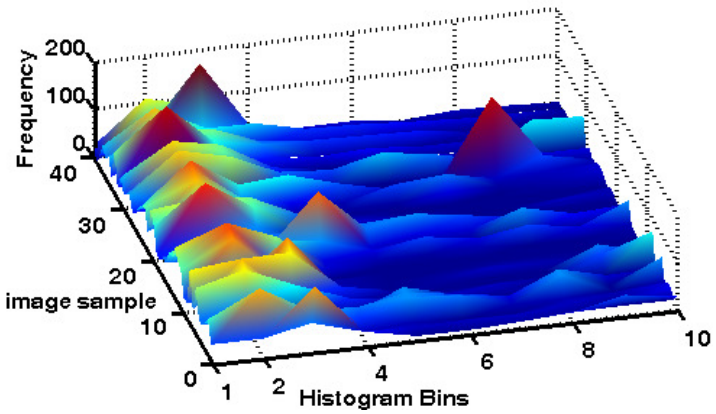

FIGURE 10: Average values of the $Ch_{1,1,1}$ component on the database

		N=4	N=8	N=12	N=16	N=18
K=15	indoor	73.5	90.5	88	85.5	83.2
	outdoor	51	69.2	80.5	89.5	82.4
K=20	indoor	78	86.5	92	87.5	88.1
	outdoor	63.5	74	80.5	89	82.2
K=30	indoor	70	85.5	90	87	87.1
	outdoor	52	72	80	87.5	77.2

TABLE 1: Results of classification on DB1

After finding the *fv* for an image, KNN classifier is used for classification. Table1 shows the result of image classification for different N (number of color channels) and K (number of neighbors in KNN classifier). From this table it can be seen N=16 yields the best result when considering both indoor and outdoor detection rates. Furthermore when K=20 is chosen, 87.5% indoor and 89% outdoor images are correctly classified. Table 2 shows the classification results on DB2. In this experiment, the results also show that choosing 16 channels for classification achieves higher classification rates. The overall comparisons on DB1 and DB2 show that results only differ by a small percentage. This shows that the method is robust for classification of images taken under unknown camera calibration and image compression.

		N=4	N=8	N=12	N=16	N=18
K=15	indoor	77	92.5	91.5	87.5	90.5
	outdoor	54	72	82.5	90	78.5
K=20	indoor	81.5	88.5	90.5	90	85.2
	outdoor	63.5	86	84.5	89.5	86.5
K=30	indoor	74	87.5	88.5	88.5	84.5
	outdoor	57	74.5	82.5	89.5	83.7

TABLE 2: Results of classification on DB2

To observe the results based on accuracy of classification and to find the K which yields the best results, fig. 11 shows the accuracy of each experiment. Based on this figure it can be seen that when DB1 and DB2 with N=16 and K=20 are chosen best classification rates with 88.25% and 89.75% in accuracy are obtained.

In Most cases, it can be seen that indoor images have been detected with more accuracy. This because the outdoor image are exposed to more diverse lighting conditions since the spectrum of sunlight is changing during daytime and also reflections from the sea, clouds and the ground makes the spectrum of the reflected light more complex.

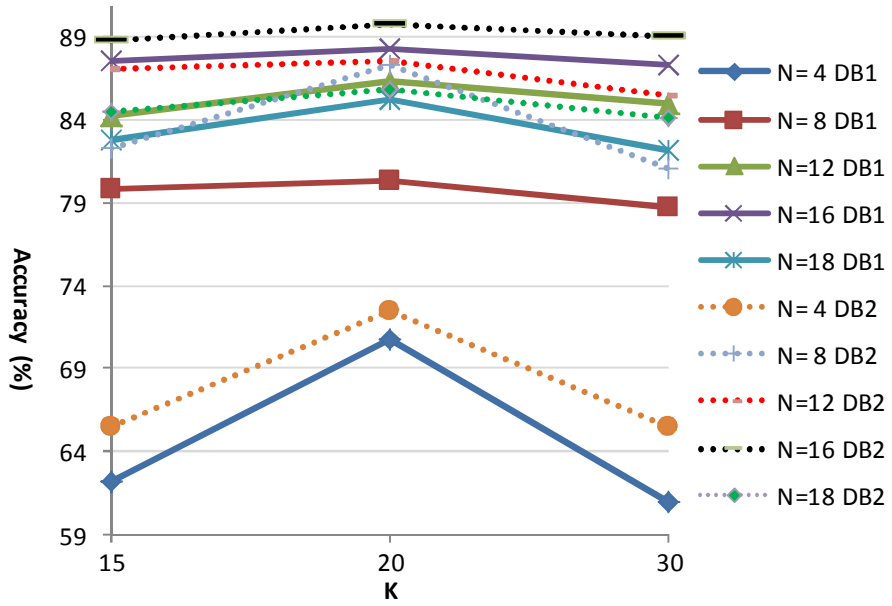

FIGURE 11: Accuracy of the all test cases

To evaluate classification accuracy of the proposed method, two color features: Color Oriented Histograms (COH) and the Ohta color space used in [15] and [3] respectively are extracted and tested on images in DB1. Table 3 shows the result of this comparison. These features are extracted as explained in the original document.

		CCT	COH	Ohta
K=15	Indoor	85.5	94	85.5
	Outdoor	89.5	68.5	70.25
	Accuracy	**87.5**	**81.25**	**78.75**
K=20	Indoor	87.5	95	84
	Outdoor	89	69.5	70
	Accuracy	**88.25**	**82.25**	**77**
K=25	Indoor	87	96.5	86
	Outdoor	87.5	68	68.5
	Accuracy	**87.25**	**82.25**	**77.25**

TABLE 3: Comparison of different methods

From the results of this table, it is clear that the proposed method outperforms the state of the art methods at least by 5%. The indoor classification rate using COH is in most cases more significant in comparison to the classification rate using CCT, but outdoor classification using COH shows quite low detection rates. Ohta color space shows not to be a preferable color space for indoor-outdoor image classification. To further investigate the robustness of the proposed method, in another experiment the result of indoor-outdoor classification is tested when the JPEG Compression Ratio (CR) is changed for image in DB1[30].

		CR=2	CR=3	CR=5	CR=10
CCT	Indoor	86	87.5	77	74.5
	Outdoor	80	76	73	67
	Accuracy	**83**	**81.75**	**75**	**70.75**
COH	Indoor	88	79.5	76	72.5
	Outdoor	62.5	60	53	54.5
	Accuracy	**75.25**	**69.75**	**64.5**	**63.5**
Ohta	Indoor	71	73.5	69.5	63
	Outdoor	69.3	67	61	54.5
	Accuracy	**70.15**	**70.25**	**65.25**	**58.75**

TABLE 4:. Effect of JPEG compression classification results

Table 4 summarizes the result of indoor-outdoor image classification for different compression rates on DB1. From this table it can be seen that the CCT of the image is less affected when CR=2 and 3 but as CR is increased the results for all methods start to degrade. For CR=10 classification accuracy based on CCT feature is still higher than 70% while for two other tested approached , they are decreased to less than 65%. This result shows the robustness of the proposed method against changes in compression changes applied to digital images.

5. CONCLUSIONS

In this paper, a new method based on image CCT was proposed for indoor-outdoor image classification. Images were first segmented into different color channels and based on the proposed algorithm CCT of each color channels was calculated. These CCTs formed the feature vector which was fed to a KNN classifier to classify images as indoor or outdoor. Tests were conducted on two datasets collected from the internet and video frames extracted from 40 different video clips. The classification results showed that incorporating CCT information yields high classification accuracy of 88.25% on DB1 and 89.75% on DB2. The result of classification on DB1 showed 5% improvement compared to other state of the art methods. In addition, the method was tested against changes in the JPEG compression rate applied to

images where the method showed to be more robust compared to other methods. High classification rate and robustness of the presented method makes it highly applicable for the application of indoor-outdoor image classification.

6. REFERENCES

[1] Angadi, S.A. and M.M. Kodabagi, *A Texture Based Methodology for Text Region Extraction from Low Resolution Natural Scene Images.* International Journal of Image Processing, 2009. **3**(5): p. 229-245.

[2] Bianco, S., et al., *Improving Color Constancy Using Indoor–Outdoor Image Classification.* IEEE transaction on Image Processing, 2008. **17**(12): p. 2381-2392.

[3] Szummer, M. and R.W. Picard, *Indoor-outdoor image classification*, in *IEEE Workshop on Content-Based Access of Image and Video Database*. 1998: Bombay, India. p. 42-51.

[4] Ohta, Y.I., T. Kanade, and T. Sakai, *Color information for region segmentation.* Computer Graphics and Image Processing, 1980. **13**(3): p. 222-241.

[5] Serrano, N., A. Savakis, and J. Luo, *A computationally efficient approach to indoor/outdoor scene classification*, in *International Conference on Pattern Recognition*. 2002: QC, Canada, . p. 146-149.

[6] Miene, A., et al., *Automatic shot boundary detection and classification of indoor and outdoor scenes*, in *Information Technology, 11th Text Retrieval Conference*. 2003, Citeseer. p. 615-620.

[7] Qiu, G., X. Feng, and J. Fang, *Compressing histogram representations for automatic colour photo categorization.* Pattern Recognition, 2004. **37**(11): p. 2177-2193.

[8] Huang, J., et al., *Image indexing using color correlograms.* International Journal of Computer Vision, 2001: p. 245–268.

[9] Qiu, G., *Indexing chromatic and achromatic patterns for content-based colour image retrieval.* Pattern Recognition, 2002. **35**(8): p. 1675-1686.

[10] Qiu, G. and K.M. Lam, *Spectrally layered color indexing.* Lecture Notes in Computer Science, 2002. **2384**: p. 100-107.

[11] Collier, J. and A. Ramirez-Serrano, *Environment Classification for Indoor/Outdoor Robotic Mapping*, in *Canadian Conference on Computer and Robot Vision*. 2009, IEEE. p. 276-283.

[12] Boutell, M. and J. Luo, *Bayesian Fusion of Camera Metadata Cues in Semantic Scene Classification*, in *Computer Vision and Pattern Recognition (CVPR)*. 2004: Washington, D.C. p. 623-630.

[13] Tao, L., Y.H. Kim, and Y.T. Kim, *An efficient neural network based indoor-outdoor scene classification algorithm*, in *International Conference on Consumer Electronics*. 2010: Las Vegas, NV p. 317-318.

[14] Vailaya, A., et al., *Image classification for content-based indexing.* IEEE Transactions on Image Processing, 2001. **10**(1): p. 117-130.

[15] Kim, W., J. Park, and C. Kim, *A Novel Method for Efficient Indoor–Outdoor Image Classification.* Signal Processing Systems, 2010. **61**(3): p. 1-8.

[16] Daubechies, I., *Ten Lectures on Wavlets*. 1992, Philadelphia: SIAM Publications.

[17] Gupta, L., et al., *Indoor versus outdoor scene classification using probabilistic neural network* Eurasip Journal on Advances in Signal Processing, 2007. **1**: p. 123-133.

[18] Tolambiya, A., S. Venkatraman, and P.K. Kalra, *Content-based image classification with wavelet relevance vector machines.* Soft Computing, 2010. **14**(2): p. 129-136.

[19] Hu, G.H., J.J. Bu, and C. Chen, *A novel Bayesian framework for indoor-outdoor image classification*, in *International Conference on Machine Learning and Cybernetics* 2003: Xian. p. 3028-3032

[20] Payne, A. and S. Singh, *Indoor vs. outdoor scene classification in digital photographs.* Pattern Recognition, 2005. **38**(10): p. 1533-1545.

[21] Songbo, T., *An effective refinement strategy for KNN text classifier.* Expert Systems with Application, 2006. **30**(2): p. 290-298.

[22] Shafer, S.A., *Using color to separate reflection components.* Color Research and Application, 1985. **10**(4): p. 210.

[23] Ebner, M., *Color constancy*. 2007, West Sussex: Wily.

[24] Finlayson, G., G. Schaefer, and S. Surface, *Single surface colour constancy*, in *7th Color Imaging Conference: Color Science, Systems, and Applications*. 1999: Scottsdale, USA. p. 106-113.

[25] Cheng, H.D., et al., *color image segmentation: advances and prospects.* Pattern Recognition, 2001. **34**(12): p. 2259-2281.

[26] WNUKOWICZ, K. and W. SKARBEK, *Colour temperature estimation algorithm for digital images - properties and convergence.* OPTO-ELECTRONICS REVIEW, 2003. **11**(3): p. 193-196.

[27] Lee, H., et al., *One-dimensional conversion of color temperature in perceived illumination.* Consumer Electronics, IEEE Transactions on, 2001. **47**(3): p. 340-346.

[28] Javier, H., J. Romero, and L.R. Lee, *Calculating correlated color temperatures across the entire gamut of daylight and skylight chromaticities.* Applied Optis, 1999. **38**(27): p. 5703-5709.

[29] Robertson, A. and R. Alan, *computation of Correlated Color Temperature abd Distribution Temperature.* Color Research and Application, 1968. **58**(11): p. 1528-1535.

[30] Yang, E. and L. Wang, *Joint optimization of run-length coding, Huffman coding, and quantization table with complete baseline JPEG decoder compatibility.* Image Processing, IEEE Transactions on, 2009. **18**(1): p. 63-74.